

1 **Non-homologous DNA increases gene disruption efficiency by altering DNA repair**  
2 **outcomes**

3  
4 **Author List**

5 Richardson, CD<sup>1,2, ‡</sup>; Ray, GJ<sup>1,2, ‡</sup>; Corn, JE<sup>1,2\*</sup>

6 <sup>1</sup>Innovative Genomics Initiative, University of California, Berkeley, 94720

7 <sup>2</sup>Department of Molecular and Cell Biology, University of California, Berkeley, CA, 94720

8 <sup>‡</sup>authors contributed equally to this work

9 \*Correspondence: [jcorn@berkeley.edu](mailto:jcorn@berkeley.edu)

10

11 **Abstract**

12 Cas9 endonuclease can be targeted to genomic sequences by varying the sequence of  
13 the single guide RNA (sgRNA). The activity of these Cas9-sgRNA combinations varies  
14 widely at different genomic loci and in different cell types. Thus, disrupting genes in  
15 polyploid cell lines, or using inefficient sgRNAs, can require extensive downstream  
16 screening to identify homozygous clones. We have found that linear, non-homologous  
17 oligonucleotide DNA greatly stimulates Cas9-mediated gene disruption in the absence of  
18 homology-directed repair. This stimulation greatly increases the frequency of clones with  
19 homozygous gene disruptions, even in polyploid cell lines, and rescues otherwise  
20 ineffective sgRNAs. The mechanism of enhanced gene disruption differs between  
21 human cell lines, stimulating deletion of genomic sequence and/or insertion of non-  
22 homologous oligonucleotide DNA at the edited locus in a cell line specific manner.  
23 Thus, the addition of non-homologous DNA appears to drive cells towards error-prone  
24 instead of error-free repair pathways, dramatically increasing the frequency of gene  
25 disruption.

26

27 **Main Text**

28 Programmable genetic disruption holds great promise for the investigation of  
29 gene function and translational potential for the treatment of many diseases. Gene  
30 knockouts are commonly generated by introducing a site specific double strand break  
31 (DSB) within the gene of interest and screening for clones in which one or more alleles  
32 have been repaired in an error-prone fashion to disrupt the open reading frame<sup>1</sup>. The  
33 efficiency of this process is limited by the number of clones that must be screened to find  
34 the interruption, which is itself a product of the frequency of genome cutting and the

35 frequency of disruptive repair events. The programmable Cas9 nuclease, which relies  
36 upon a targeting single guide RNA (sgRNA), has recently emerged as a popular tool for  
37 gene disruption due to its relative ease of use<sup>2</sup>. But Cas9-sgRNA combinations vary  
38 greatly in apparent cellular activity, from completely inactive to nearly 100% efficient,  
39 which can complicate experiments in which functional concerns place restrictions on the  
40 location to be targeted<sup>3-6</sup>. This variable activity has been attributed to differences in  
41 Cas9's ability to use sgRNAs of various sequences<sup>7,8</sup>, but differences in the activity of a  
42 given sgRNA between cell lines and organisms suggests that location- or organism-  
43 specific modulation of DNA repair outcomes may influence observed sgRNA efficiency.  
44 Here we show that the addition of linear DNA, including non-homologous sequences,  
45 during Cas9-mediated gene ablation greatly increases the frequency of disrupting  
46 mutations in multiple human cell lines. Consequently, we dramatically increase the  
47 number of cells with homozygous gene disruptions within the edited population.

48

49 While investigating parameters to optimize rates of homology directed repair  
50 (HDR) during genome editing experiments, we found that the frequency of error-prone  
51 repair outcomes also tended to increase when single stranded HDR donor DNA was  
52 present in the editing reaction<sup>9</sup>. Prompted by this observation, we undertook a  
53 systematic exploration of the parameters underlying DNA-mediated stimulation of error-  
54 prone repair events. To avoid confounding effects stemming from the use of plasmid or  
55 other nucleic acid mediated delivery of Cas9, we performed editing experiments using  
56 nucleofection to directly introduce a ribonucleoprotein complex of Cas9 complexed with  
57 sgRNA (RNP) into cells<sup>3,6</sup>.

58

59 Targeting the EMX1 locus, we selected a sub-optimal RNP whose activity was  
60 approximately 20% in HEK293T cells. We found that the addition of a 127-mer single  
61 stranded DNA oligonucleotide derived from BFP, which lacks homology to the targeted  
62 locus and whose sequence is absent in the human genome, dramatically increased the  
63 appearance of insertions and deletions (indels) as measured by a T7E1 assay (**Figure**  
64 **1A**). We henceforth refer to such non-homologous oligonucleotides as "N-oligos". The  
65 ability of N-oligos to increase editing efficiency was titratable and depended upon oligo  
66 length, with shorter oligos losing efficacy. Native and denatured salmon sperm DNA  
67 were also capable of stimulating indels to a similar extent as synthetic single stranded  
68 oligonucleotides. Neither the charged agents Heparin and Spermidine (**Extended Data**

69 **Figure 1**), nor dl-dC had little effect on editing, indicating that complex nucleic acid was  
70 necessary for stimulation. Free DNA ends were also required, as closed circular plasmid  
71 was ineffective. Importantly, DNA-mediated stimulation of indel formation is specific to  
72 the targeted site and does not increase editing at predicted off-target sites as measured  
73 by TIDE analysis<sup>10-11</sup> (**Extended Data Figure 2**).

74

75 We next asked whether the use of N-oligos to increase editing could be  
76 generalized to different cell types and genomic loci. We found that N-oligos stimulated  
77 indel formation in five out of the seven cell lines tested, with tissue types ranging from  
78 bone to blood, including a five-fold increase in indels in U2OS cells (**Figure 1B**). N-oligo  
79 stimulation of indels was observed at the YOD1 and JOSD1 loci. This stimulation at the  
80 YOD1 locus “rescued” an otherwise completely ineffective guide, more than doubling the  
81 rate of indel formation from nearly undetectable to approximately 17% (**Extended Data**  
82 **Figure 3**).

83

84 Because the T7E1 indel formation assay operates on an edited pool of cells and  
85 does not report on individual alleles, we used TA/TOPO cloning and Sanger sequencing  
86 to determine if increased indel frequency corresponded to a higher number of clonal  
87 homozygous knockouts. We focused on HEK293T cells, which have a tetraploid genome  
88 and are thus a stringent test case for the formation of homozygous knockouts.  
89 Characterizing clonally isolated edited cells, we found that editing with RNP alone  
90 yielded 40% heterozygous clones and no homozygous knockouts, whereas RNP with N-  
91 oligos yielded 40% heterozygotes and 60% homozygous knockouts (**Figure 1C**). Hence,  
92 the use of N-oligos is a simple and effective technique to increase the frequency of  
93 homozygous gene disruption.

94

95 Sequence analysis of the alleles in HEK293 editing reactions revealed that N-  
96 oligo treatment increased the rate of both insertions and deletions relative to RNP  
97 treatment alone (**Figure 2A**). These indels included simple deletion of sequence around  
98 the cut site and insertion of random sequence, but surprisingly also insertion of N-oligo  
99 sequence and insertion of the DNA template used for *in vitro* transcription of the sgRNA  
100 (example indels, **Figure 2B**; all indels **Extended Data Figure 4**). The frequent presence  
101 of sgRNA template sequence was particularly striking, as the N-oligo was approximately  
102 1000-fold more abundant in the nucleofection reactions (**Extended Data Figure 5**). The

103 occasional insertion of non homologous DNA into double strand breaks has been  
104 reported in yeast<sup>12-14</sup> and mice<sup>15-17</sup> and the insertion of short phosphorothioate-protected  
105 oligos forms the basis of the GUIDE-Seq method to detect off-target genome editing  
106 events<sup>18</sup>, but the ability of non-homologous single stranded DNA to greatly increase  
107 gene knockout by stimulating these events is surprising and to the best of our knowledge  
108 unprecedented.

109

110 Our observations of sequence insertion in HEK293T cells motivated us to  
111 investigate the nature of N-oligo stimulated indel formation in other cell types.  
112 Surprisingly, Sanger sequencing of U2OS editing outcomes revealed that N-oligo  
113 treatment primarily stimulated the appearance of large deletions, and not insertions, as  
114 compared to RNP alone editing (**Figure 2C**). To determine the propensity of various cell  
115 types to insert sequences into a Cas9 break point, we designed a PCR assay to amplify  
116 either the N-oligo or sgRNA transcription template in various orientations. This assay  
117 confirmed sequence insertion in K562 and HEK293T cells, but not in any of the other cell  
118 lines that show robust N-oligo indel stimulation (**Figures 2D, 1B**). The ability of N-oligos  
119 to stimulate gene disruption with such different molecular outcomes suggests that they  
120 stimulate classical or alternative end-joining pathways<sup>19</sup>, thereby boosting the rate of  
121 error-prone DSB repair.

122

123 Given the large excess of N-oligo over sgRNA template, we wondered if  
124 providing high concentrations of double stranded non-homologous DNA would also  
125 effectively stimulate insertion in these cells. We tested both single and double stranded  
126 N-oligos for their potential to increase indels at the EMX1 locus, double purifying the  
127 sgRNA before use to ensure that the double stranded sgRNA template was completely  
128 removed. We found that double stranded N-oligo stimulated indels, though about two-  
129 fold less effectively than single stranded N-oligo (**Extended Data Figure 6A**). Using a  
130 PCR assay for sequence integration, we found no evidence of sgRNA template insertion  
131 in doubly-purified samples, but greater integration of the duplex N-oligo relative to single-  
132 stranded N-oligo (**Extended Data Figure 6B**). This result suggests that explicitly  
133 designing a duplex N-oligo could further bias cells towards a specific outcome, for  
134 example inserting a cassette that encodes stop codons in multiple frames and  
135 orientations may further bias cells towards a specific repair outcome. This strategy has

136 been proposed for HDR-mediated gene disruption, but to our knowledge has not been  
137 attempted with non-homologous integration of oligonucleotides<sup>20</sup>.

138

139 Taken together, our data support a model in which cells faithfully repair most  
140 Cas9-generated DSBs using error-free repair pathways that do not produce measurable  
141 indels, but occasional error-prone repair causes indels that ablate portions of the Cas9  
142 protospacer and/or PAM, thereby preventing further cutting and producing a measurable  
143 outcome (**Extended Data Figure 7**). We note that if repair outcomes depend upon  
144 sequence context, this activity could cause Cas9-sgRNA combinations with high *in vitro*  
145 activity to display poor cellular activity or for sgRNA activity to differ between cell lines<sup>7,8</sup>.  
146 The addition of N-oligo during editing appears to stimulate error-prone end-joining  
147 pathways that differ among cell types (e.g. end-joining of exogenous nucleic acid in  
148 HEK293T and large deletions in U2OS) but have the net effect of increasing the rate of  
149 gene disruption. We anticipate that the use of N-oligos will be extremely valuable in  
150 generating homozygously gene-disrupted cell lines or organisms, and will be particularly  
151 effective in challenging polyploid contexts.

152

### 153 **Figure Legends**

154 • **Figure 1:** Nonhomologous DNA increases gene disruption in multiple cell types.  
155 (A) Single and double stranded linear nonhomologous DNA stimulates indel  
156 formation in HEK293 cells. Cas9 was targeted to the EMX1 locus with or without  
157 nucleic acid carrier agents (-, no nucleic acid). Indel formation was measured  
158 using a T7 endonuclease I assay (mean  $\pm$  standard deviation of at least two  
159 independent experiments, gels presented in **Document S1**). (B) N-oligo DNA  
160 boosts editing rates in multiple cell types. Editing was performed as described in  
161 panel A in multiple cell types either with (dark grey bars) or without (light gray  
162 bars) 4.5ug of N-oligo. (C) N-oligo increases the frequency of homozygous gene  
163 disruption. HEK293 cells edited in panel B were clonally isolated and amplicons  
164 were sequenced to determine genotype. Each horizontal bar represents a single  
165 clone with green (wildtype sequence) or magenta (mutations disrupting EMX1)  
166 divisions sized according to the percentage of sequencing reads in each  
167 category. Zygosity is summarized in the lower table.

168

169 • **Figure 2:** N-oligo stimulation of gene disruption promotes error-prone repair  
170 events. **(A)** N-oligo stimulates insertions and deletions in HEK293 cells. The  
171 allele frequency of deletions (left, green) and insertions (blue, right) are shown for  
172 nucleofections performed with or without N-oligo. Editing is summarized for each  
173 clone in **Extended Data Figure 4**. Raw data is available in **Document S3**. **(B)**  
174 Inserted sequences are derived from single and double stranded heterologous  
175 DNA. Wildtype EMX1 sequence is presented at top with the protospacer (bold),  
176 PAM (bold underline), and cut site (triangle) diagrammed. Four example alleles  
177 are presented below with sgRNA template (green) and/or N-oligo (blue)  
178 sequence inserted in both orientations. Complete sequencing alignments are  
179 available in Document S3. **(C)** N-oligo stimulates deletions in U2OS cells.  
180 Multiple sequence reads from edited cell populations are presented as described  
181 in **Figure 2A**. **(D)** Insertion of nonhomologous DNA primarily occurs in HEK293  
182 and K562 cells. DNA harvested from edited cell populations was evaluated using  
183 a panel of PCR reactions (diagrammed at top). Primers N1 and N2 anneal to the  
184 N-oligo sequence; primers T1 and T2 anneal to residual sgRNA template.

185  
186

### 187 **Supplemental Documents**

- 188 • **Document S1:** Uncropped gels from Figures 1A, 1B, 2D, and Extended 6.
- 189 • **Document S2:** Sequences of constructs/PCR primers/etc
- 190 • **Document S3:** Sequences for all clones/reads

191

192

### 193 **Materials and Methods**

#### 194 Cell Lines and Cell Culture

195 A-431, HEK293, HeLa, Jurkat, K562, MDA-MB-231, and U2OS cells were acquired from  
196 the UC Berkeley Tissue Culture Facility. A-431, HeLa, and MDA-MB-231 cells were  
197 maintained in DMEM glutamax medium supplemented with 10% fetal bovine serum, 1%  
198 sodium pyruvate, 1% non-essential amino acids, and 100 ug/mL penicillin-streptomycin.  
199 HEK293 and U2OS cells were maintained in DMEM medium supplemented with 10%  
200 fetal bovine serum, 1% sodium pyruvate, and 100 ug/mL penicillin-streptomycin. Jurkat  
201 and K562 cells were maintained in RPMI medium supplemented with 10% fetal bovine  
202 serum, 1% sodium pyruvate, and 100 ug/mL penicillin-streptomycin.

203

#### 204 Cas9 and RNA Preparation

205 *S. pyogenes* Cas9 (pMJ915, Addgene #) with two nuclear localization signal peptides  
206 and an HA tag at the C-terminus were purified by a combination of affinity, ion exchange,  
207 and size exclusion chromatography steps as described<sup>21</sup>, except protein was eluted at  
208 40uM in 20 mM HEPES KOH pH 7.5, 5% glycerol, 150 mM KCl, 1 mM DTT.

209

210 sgRNAs were generated by HiScribe (NEB E2050S) T7 in vitro transcription using PCR-  
211 generated DNA as a template ([dx.doi.org/10.17504/protocols.io.dm749m](https://doi.org/10.17504/protocols.io.dm749m)). Complete  
212 sequences for all sgRNA templates can be found in Document S2.

213

#### 214 Cas9 RNP Assembly and Nucleofection

215 100 pmoles of Cas9-2NLS was diluted to a final volume of 5uL with Cas9 buffer (20 mM  
216 HEPES (pH 7.5), 150 mM KCl, 1 mM MgCl<sub>2</sub>, 10% glycerol and 1 mM TCEP) and mixed  
217 slowly into 5uL of Cas9 buffer containing 120 pmoles of L2 sgRNA. The resulting mixture  
218 was incubated for ten minutes at room temperature to allow RNP formation. 2E+05 cells  
219 were harvested, washed once in PBS, and resuspended in 20uL of nucleofection buffer  
220 (Lonza, Basel, Switzerland). 10uL of RNP mixture, 4.5 uL of N-oligo, and cell suspension  
221 were combined in a Lonza 4d strip nucleocuvette. Reaction mixtures were  
222 electroporated, incubated in the nucleocuvette at RT for ten minutes, and transferred to  
223 culture dishes containing pre-warmed media ([dx.doi.org/10.17504/protocols.io.dm649d](https://doi.org/10.17504/protocols.io.dm649d)).  
224 Editing outcomes were measured two days post-nucleofection by T7E1 (see below).  
225 Resuspension buffer and electroporation conditions were the following for each cell line:  
226 A-431 in SF with EQ-100, HEK293 in SF with DS-150, HeLa in SE with CN-114, Jurkat  
227 in SE with CL-120, K562 in SF with FF-120, MDA-MB-231 in SE with CH-125, and  
228 U2OS in SE with CM104.

229

230

#### 231 PCR Amplification of Edited Regions

232 PCR amplification of EMX1 was done using primers oCR295 and oCR296. PCR  
233 amplification of YOD1 was done using YOD1f and YOD1r. PCR amplification of JOSD1  
234 was done using JOSD1f and JOSD1r. PCR reactions were performed with 200 ng of  
235 genomic DNA and Kapa Hot Start high-fidelity polymerase with the GC buffer. The

236 thermocycler was set for one cycle of 95°C for 5 min, 30 cycles of 98°C for 20 sec, 62°C  
237 for 15 sec, 72°C for 30 sec, and one cycle of 72°C for 1 min, and held at 4°C.

238

#### 239 T7EI Assay

240 The rate of Cas9 mediated gene disruption was measured by T7 endonuclease I  
241 digestion of hybridized PCR. 200 ng of PCR DNA in 1X NEB Buffer 2 was hybridized in  
242 a thermocycler under the following conditions: 95°C for 5 min, 95-85°C at -2°C/sec, 85-  
243 25°C at -.1°C/sec, and held at 4°C. 10 units of T7EI (NEB, M0302) were added to the  
244 sample and was incubated at 37°C for 15 min. The sample was then immediately run on  
245 a 2% agarose gel containing ethidium bromide. Band intensities were quantified by  
246 imageJ. Indel percentage was calculated using the following equation:  $(1 - (1 - (\text{cut product}$   
247  $\text{intensities} / \text{uncut} + \text{cut product intensities}))^{1/2}) \times 100^5$ .

248

#### 249 Insert Based PCR Assay

250 To assay the insertion of N-oligo and sgRNA template DNA into the cut site, a reverse  
251 primer (oGJR102) was designed to pair with forward primers homologous to the: BFP N-  
252 oligo inserted in the forward direction (oGJR097), BFP N-oligo inserted in the reverse  
253 direction (oGJR098), the T7 promoter of the sgRNA template inserted in the forward  
254 direction (oGJR099), and the T7 promoter of the sgRNA template inserted in the reverse  
255 direction (oGJR100). Presence of EMX1 DNA in the PCR reaction was verified using the  
256 EMX1 PCR performed above. PCR reactions were performed with 200 ng of genomic  
257 DNA and Kapa Hot Start high-fidelity polymerase. The thermocycler was set for one  
258 cycle of 95°C for 5 min, 30 cycles of 98°C for 20 sec, 64°C for 15 sec, 72°C for 30 sec,  
259 and one cycle of 72°C for 1 min, and held at 4°C. The sample was then run on a 2%  
260 agarose gel containing ethidium bromide.

261

#### 262 qPCR on RNP

263 sgRNA template and N-oligo DNA present in the nucleofection reaction mixture was  
264 quantified on a Mastercycler 2 qPCR machine (Eppendorf, Hamburg). Primers oCR427  
265 and oCR428, sgRNA template; oGJR103 and oGJR104, N-oligo; **Document S2** were  
266 used at a final concentration of 500nM in Power SYBR green reaction mixture (Thermo  
267 Fisher). Reaction conditions were 95°C for 10 minutes followed by 40 cycles of 95°C for  
268 30 seconds and 65°C for 60 seconds. The ratio of N-oligo to sgRNA template was

269 quantified using the equation  $r=2^{(Ct_{\text{sgRNA}}-Ct_{\text{N-oligo}})}$ . Ratios from three serial dilutions of  
270 template DNA were averaged and presented as mean  $\pm$  standard deviation.

271

## 272 TIDE Analysis

273 Off-target analysis was performed on the top 4 targets given by the online tool available  
274 at <http://crispr.mit.edu><sup>22</sup>. Sequences are presented in **Extended Data Figure 2** and  
275 **Document S2**. Genomic sequences were amplified using KAPA polymerase and  
276 Sanger sequenced by the UC Berkeley Sequencing Core. PCR reactions were  
277 performed using 200 ng of genomic DNA and the thermocycler was set for one cycle of  
278 95°C for 5 min, 30 cycles of 98°C for 20 sec, the annealing temperature for 15 sec, 72°C  
279 for 30 sec, and one cycle of 72°C for 1 min, and held at 4°C. Off-Target 1 PCR was  
280 done with oGJR051 and oGJR096 with a 64°C annealing temperature, off-Target 2 PCR  
281 was done with oGJR090 and oGJR091 with a 62°C annealing temperature, off-Target 3  
282 PCR was done with oGJR053 and oGJR071 with a 64°C annealing temperature, and  
283 off-Target 4 PCR was done with oGJR054 and oGJR072 with a 66°C annealing  
284 temperature. ABIF files were uploaded to <http://www.tide.nki.nl> for analysis<sup>11</sup>.

285

## 286 **Acknowledgments**

287 We thank members of the Corn lab for helpful discussions on this manuscript. This work  
288 was supported by the Li Ka Shing Foundation.

289

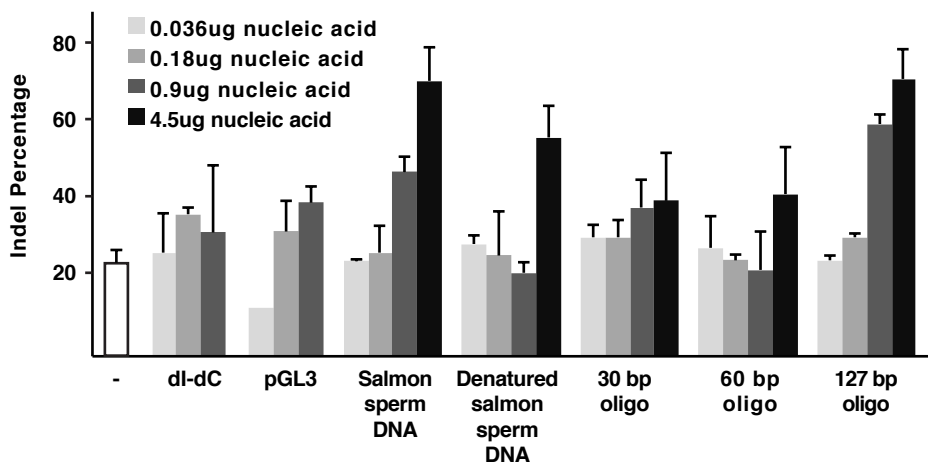
## 290 **References**

- 291 1. Yang, L., Yang, J. L., Byrne, S., Pan, J. & Church, G. M. CRISPR/Cas9-Directed  
292 Genome Editing of Cultured Cells. *Current protocols in molecular biology / edited*  
293 *by Frederick M Ausubel [et al]* **107**, 31.1.1–31.1.17 (2014).
- 294 2. Doudna, J. A. & Charpentier, E. Genome editing. The new frontier of genome  
295 engineering with CRISPR-Cas9. *Science* **346**, 1258096 (2014).
- 296 3. Lin, S., Staahl, B. T., Alla, R. K. & Doudna, J. A. Enhanced homology-directed  
297 human genome engineering by controlled timing of CRISPR/Cas9 delivery. *eLife*  
298 **4**, (2014).
- 299 4. Yang, L. *et al.* Optimization of scarless human stem cell genome editing. *Nucleic*  
300 *Acids Research* **41**, 9049–9061 (2013).
- 301 5. Ran, F. A. *et al.* Double nicking by RNA-guided CRISPR Cas9 for enhanced  
302 genome editing specificity. *Cell* **154**, 1380–1389 (2013).
- 303 6. Kim, S., Kim, D., Cho, S. W., Kim, J. & Kim, J.-S. Highly efficient RNA-guided  
304 genome editing in human cells via delivery of purified Cas9 ribonucleoproteins.  
305 *Genome Research* **24**, 1012–1019 (2014).
- 306 7. Doench, J. G. *et al.* Rational design of highly active sgRNAs for CRISPR-Cas9-  
307 mediated gene inactivation. *Nat Biotechnol* **32**, 1262–1267 (2014).
- 308 8. Moreno-Mateos, M. A. *et al.* CRISPRscan: designing highly efficient sgRNAs for

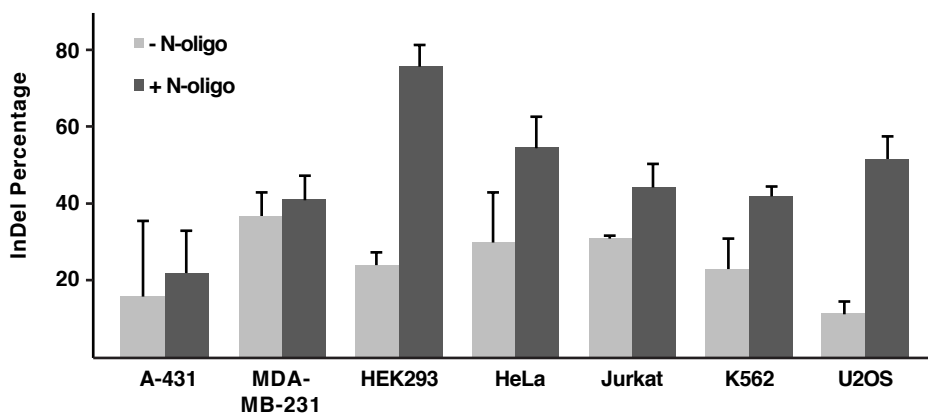
- 309 CRISPR-Cas9 targeting in vivo. *Nat Meth* **12**, 982–988 (2015).  
310 9. Richardson, C. D., Ray, G. J., DeWitt, M. A., Curie, G. L. & Corn, J. E. Enhancing  
311 homology-directed genome editing by catalytically active and inactive CRISPR-  
312 Cas9 using asymmetric donor DNA. *Nat Biotechnol* (2016). doi:10.1038/nbt.3481  
313 10. Hsu, P. D. *et al.* DNA targeting specificity of RNA-guided Cas9 nucleases. *Nat*  
314 *Biotechnol* **31**, 827–832 (2013).  
315 11. Brinkman, E. K., Chen, T., Amendola, M. & van Steensel, B. Easy quantitative  
316 assessment of genome editing by sequence trace decomposition. *Nucleic Acids*  
317 *Research* **42**, e168 (2014).  
318 12. Moore, J. K. & Haber, J. E. Capture of retrotransposon DNA at the sites of  
319 chromosomal double-strand breaks. *Nature* **383**, 644–646 (1996).  
320 13. Teng, S. C., Kim, B. & Gabriel, A. Retrotransposon reverse-transcriptase-  
321 mediated repair of chromosomal breaks. *Nature* **383**, 641–644 (1996).  
322 14. Haviv-Chesner, A., Kobayashi, Y., Gabriel, A. & Kupiec, M. Capture of linear  
323 fragments at a double-strand break in yeast. *Nucleic Acids Research* **35**, 5192–  
324 5202 (2007).  
325 15. Lin, Y. & Waldman, A. S. Promiscuous patching of broken chromosomes in  
326 mammalian cells with extrachromosomal DNA. *Nucleic Acids Research* **29**, 3975–  
327 3981 (2001).  
328 16. Onozawa, M. *et al.* Repair of DNA double-strand breaks by templated nucleotide  
329 sequence insertions derived from distant regions of the genome. *Proceedings of*  
330 *the National Academy of Sciences* **111**, 7729–7734 (2014).  
331 17. Ono, R. *et al.* Double strand break repair by capture of retrotransposon  
332 sequences and reverse-transcribed spliced mRNA sequences in mouse zygotes.  
333 *Sci Rep* **5**, 12281 (2015).  
334 18. Tsai, S. Q. *et al.* GUIDE-seq enables genome-wide profiling of off-target cleavage  
335 by CRISPR-Cas nucleases. *Nat Biotechnol* **33**, 187–197 (2015).  
336 19. Sfeir, A. & Symington, L. S. Microhomology-Mediated End Joining: A Back-up  
337 Survival Mechanism or Dedicated Pathway? *Trends Biochem Sci* **40**, 701–714  
338 (2015).  
339 20. Gagnon, J. A. *et al.* Efficient mutagenesis by Cas9 protein-mediated  
340 oligonucleotide insertion and large-scale assessment of single-guide RNAs. *PLoS*  
341 *ONE* **9**, e98186 (2014).  
342 21. Jinek, M. *et al.* A Programmable Dual-RNA-Guided DNA Endonuclease in  
343 Adaptive Bacterial Immunity. *Science* **337**, 816–821 (2012).  
344 22. Hsu, P. D., Lander, E. S. & Zhang, F. Development and applications of CRISPR-  
345 Cas9 for genome engineering. *Cell* **157**, 1262–1278 (2014).  
346

# Figure 1

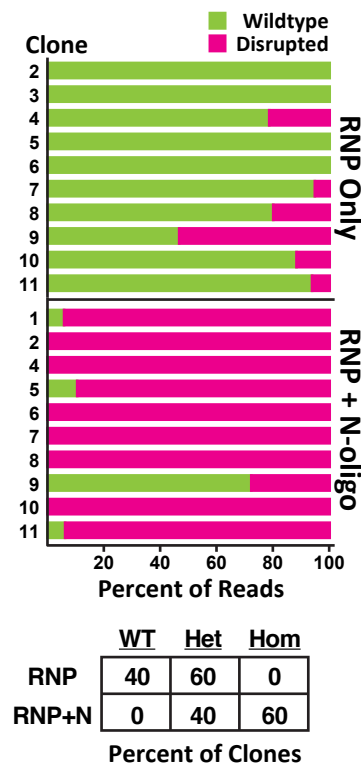
**A**



**B**



**C**

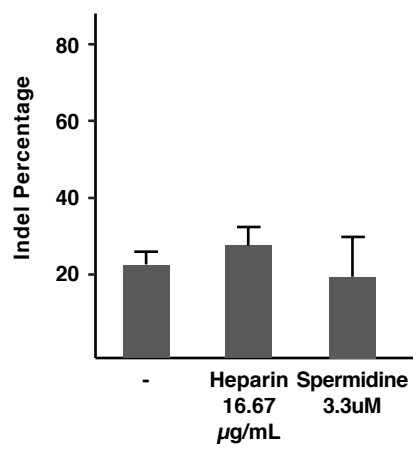


	WT	Het	Hom
RNP	40	60	0
RNP+N	0	40	60

Percent of Clones



# Extended Data Figure 1



**Extended Data Figure 1:** Heparin and spermidine do not stimulate editing at the EMX1 locus in HEK293T cells. Editing was performed as described in Figure 1A.

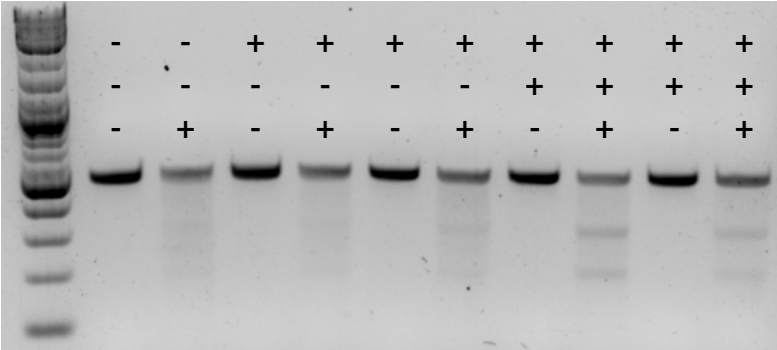
## Extended Data Figure 2

<u>Site</u>	<u>N-Oligo</u>		<u>Coordinate</u>	<u>Sequence</u>
	-	+		
<b>EMX1</b>	<b>21.4</b>	<b>55.3</b>	Chr2:72933982	CGATGTCACCTCCAATGACTAGG
<b>OT1</b>	3.2 <sup>N/S</sup>	2.3 <sup>N/S</sup>	Chr3:162729293	TAATGTCACCCCAATGACTTAG
<b>OT2</b>	2.1 <sup>N/S</sup>	1.5 <sup>N/S</sup>	Chr2:124751516	ACAAGTCACTTCCAATGACTTAG
<b>OT3</b>	1.1 <sup>N/S</sup>	2.5 <sup>N/S</sup>	Chr11:84360095	CGATTTCTCCTCCAATGATTCAG
<b>OT4</b>	1.2 <sup>N/S</sup>	1.6 <sup>N/S</sup>	Chr2:230900416	TAATATTACCTCCAATGACTCGG

**Extended Data Figure 2:** N-oligo does not stimulate measurable editing at predicted off-target sites. TIDE analysis<sup>10</sup> was performed at EMX1 and four predicted off-target sites<sup>20</sup> following editing experiments performed in the presence or absence of 4.5ug of salmon sperm DNA. Total efficiency is presented for each case. N/S – not significant, apparent editing at this locus was not significant relative to background.

# Extended Data Figure 3

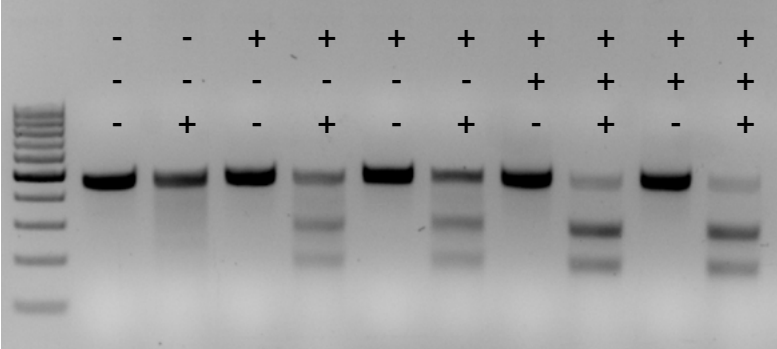
## YOD1 Locus



RNP  
N-oligo  
T7

2 4 17 8 % Indel

## JOSD1 Locus



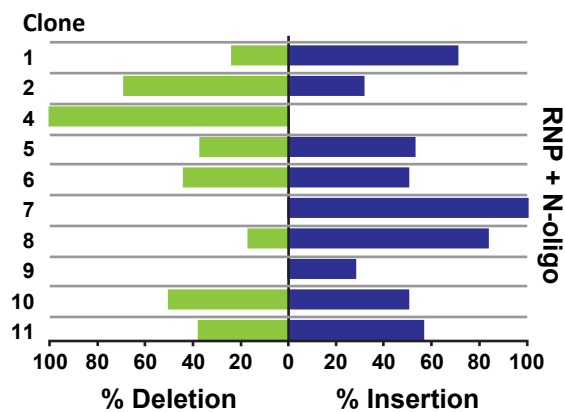
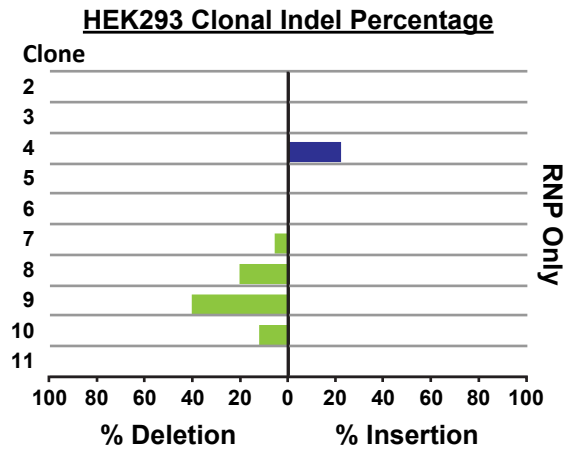
RNP  
N-oligo  
T7

26 26 55 58 % Indel

**Extended Data Figure 3:** N-oligo stimulates editing at the YOD1 and JOSD1 loci in HEK293 cells. Editing experiments were performed with or without N-oligo as indicated. Indel percentage was assayed by T7 endonuclease cleavage and gel densitometry.

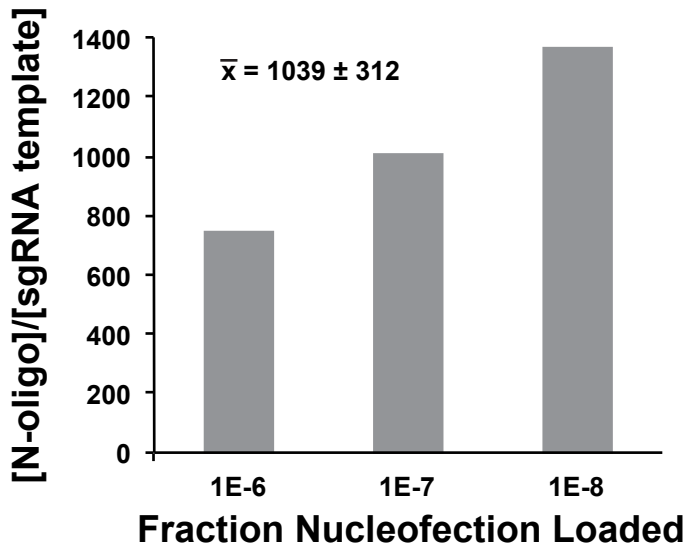
# Extended Data Figure 4

	Clone	WT	Deletions	Insertions
HEK293 RNP Only	2	(19)		
	3	(16)		
	4	(11)		9bp/2bp template indel (3)
	5	(19)		
	6	(19)		
	7	(18)	216bp del (1)	
	8	(12)	21bp del (1), 295bp del (1), 433bp del (1)	
	9	(7)	3bp del (6)	
	10	(15)	7bp del (1), 21bp del (1)	
	11	(16)		
	HEK293 RNP+N-oligo	1	(1)	3bp del (3), 5bp del (1)
2			15bp del (11)	5bp/26bp indel (5)
4			7bp del (20)	
5		(2)	5bp del (7)	11bp/5bp indel (2), 339bp/5bp template/N-oligo indel (8)
6			10bp del (7)	251bp template ins (8)
7				86bp/14bp N-oligo indel (10)
8			8bp del (2)	20bp/1bp indel (8)
9		(13)		7bp ins (10)
10			19bp del (7)	10bp/4bp indel (5)
11		(1)		119bp template ins (7)
UZOS		RNP	(56)	186bp del (1)
	RNP+ N-oligo	(9)	1-10bp del (8), 20-60bp del (5)	8bp ins (1)



**Extended Data Figure 4:** N-oligo stimulates insertions and deletions in HEK293 cells. Sequence reads from clonal cell populations were binned into three categories (WT, unmodified; deletions, clear removal of sequence; and insertions, added sequence with or without flanking deletions) and presented in table form. The complete sequence of each read can be found in Document S3. Bar graphs present clonal indel percentages.

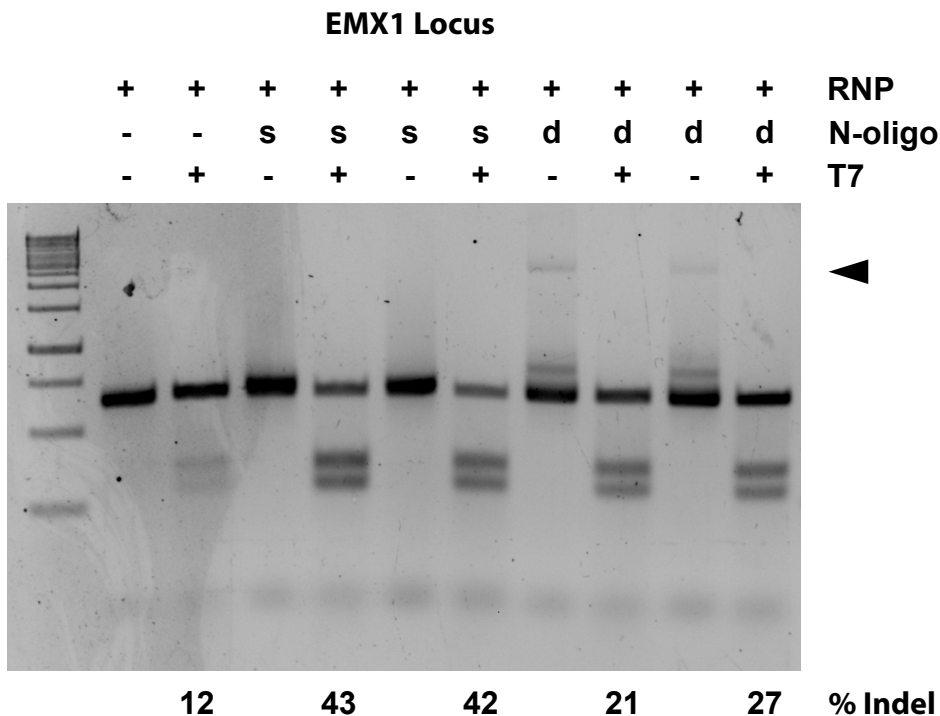
## Extended Data Figure 5



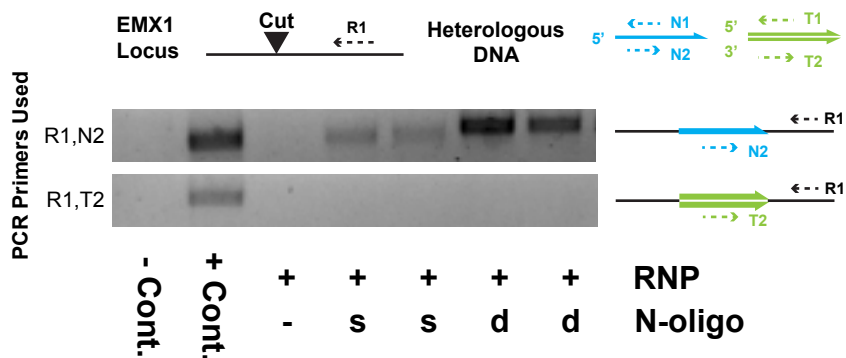
**Extended Data Figure 5:** N-oligo is present in excess of sgRNA template. Nucleofection mixtures were serially diluted and the abundance of N-oligo or sgRNA template were quantified by qPCR. Fold enrichment of N-oligo over sgRNA template are presented for three serial dilutions of nucleofection mixtures. Inset number is the mean +/- standard deviation of these three values.

# Extended Data Figure 6

**A**

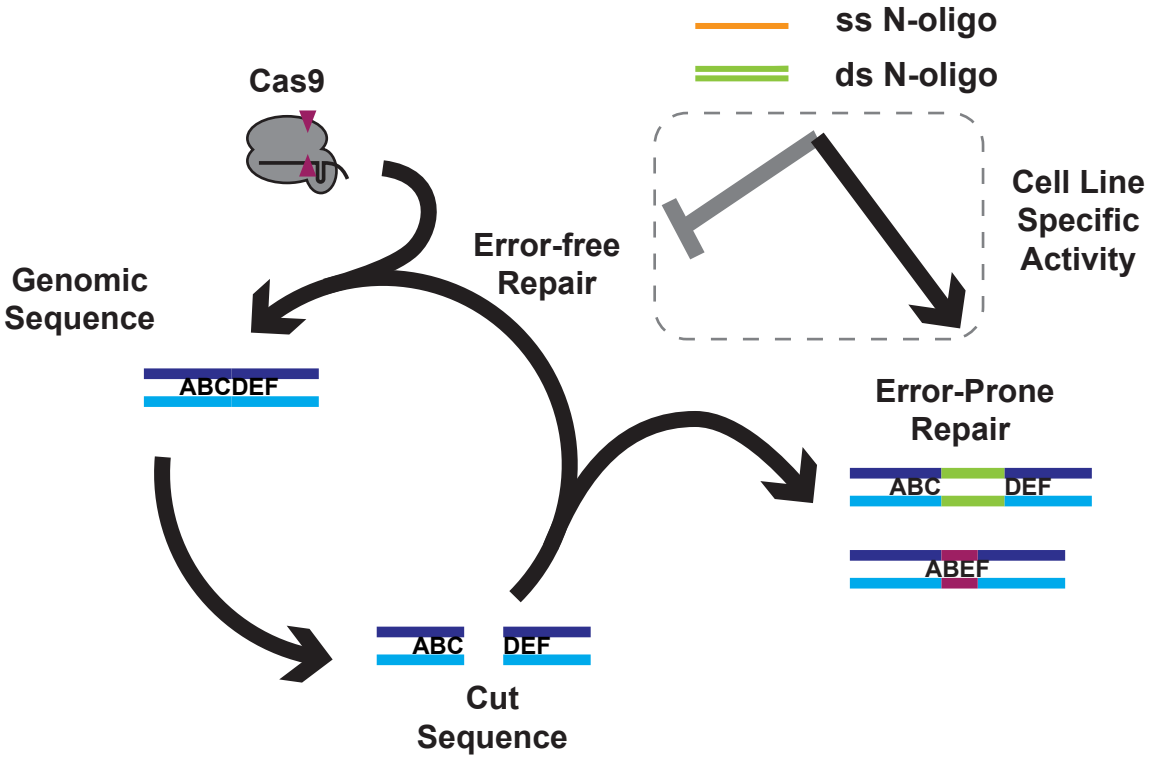


**B**



**Extended Data Figure 6:** sgRNA template DNA is not required for N-oligo increases to gene disruption. (A) Extensively purified sgRNA (free of sgRNA template DNA) was used in editing experiments at the EMX1 locus. T7 editing rates increased dramatically with the addition of single or double stranded DNA. (B) PCR for N-oligo or sgRNA template insertion indicates that insertion events are derived from the N-oligo rather than the sgRNA template. Double stranded N-oligos (d) tend to insert more efficiently than single stranded N-oligos (s).

# Extended Data Figure 7



**Extended Data Figure 7: Model for N-oligo action.** Cas9-sgRNA (grey) recognizes and cuts genomic sequence (ABCDEF). Cellular repair processes reseal most breaks in an error-free fashion, which restores the Cas9 recognition sequence and permits additional rounds of cutting. Error-prone repair events such as insertions (green sequence) and deletions (maroon region) disrupt the Cas9 recognition sequence and prevent cutting. Single and double stranded N-oligo act to inhibit error-free repair and promote error-prone repair events. Error-prone repair events stimulated by N-oligo are cell-line dependent.